Environmental Science & Technology

Article

Cite This: Environ. Sci. Technol. 2017, 51, 13494-13501

pubs.acs.org/est

Microbial Photoelectrosynthesis for Self-Sustaining Hydrogen Generation

Lu Lu,[†] Nicholas B. Williams,[‡] John A. Turner,[§] Pin-Ching Maness,[§,⊥] Jing Gu,*[,‡] and Zhiyong Jason Ren*[,†]

[†]Department of Civil, Environmental, and Architectural Engineering, University of Colorado Boulder, Boulder, Colorado 80309, United States

[‡]Department of Chemistry and Biochemistry, San Diego State University, 5500 Campanile Drive, San Diego, California 92182, United States

[§]National Renewable Energy Laboratory, Chemistry and Nanoscience Center, Golden, Colorado 80401, United States

[⊥]National Renewable Energy Laboratory, Biosciences Center, Golden, Colorado 80401, United States

Supporting Information

ABSTRACT: Current artificial photosynthesis (APS) systems are promising for the storage of solar energy via transportable and storable fuels, but the anodic half-reaction of water oxidation is an energy intensive process which in many cases poorly couples with the cathodic half-reaction. Here we demonstrate a self-sustaining microbial photoelectrosynthesis (MPES) system that pairs microbial electrochemical oxidation with photoelectrochemical water reduction for energy efficient H_2 generation. MPES reduces the overall energy requirements thereby greatly expanding the range of semiconductors that can be utilized in APS. Due to the recovery of chemical energy from waste organics by the mild microbial process and utilization of cost-effective and stable catalyst/electrode materials, our MPES system produced a stable current of 0.4 mA/cm^2 for 24 h without any external bias and ~10 mA/cm^2 with a modest bias under one sun illumination. This system also showed other merits, such as creating benefits of wastewater treatment and facile preparation and scalability.

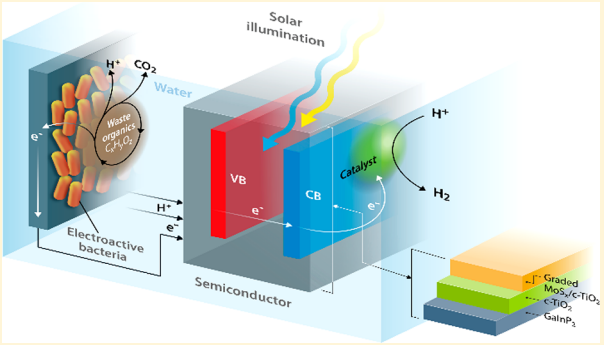

INTRODUCTION

Sunlight offers an inexhaustible and sustainable source of renewable energy to meet our increasing energy demand. Presently with the availability of low-cost solar panels, the direct harvesting of solar energy is becoming widespread, however powering society's 24-h demand is still challenging due to the variation of natural sunlight and its intermittent nature. Storage of solar energy into transportable and storable fuels, such as H_2, through the direct photoelectrolysis of water at the interface of semiconductor and electrolyte is promising for commercial utilization of solar energy.[1,2] This artificial photosynthesis (APS) system has advantages of low cost, high efficiency, as well as independence of arable land and a flexibility for tailored processes compared to natural photosynthesis.[3,4] However, the lack of a stable and efficient light-absorption semiconductor with suitable energetics remains a major challenge for water-splitting through the photoelectrochemical (PEC) approach. For example, semiconductors, such as Si, InP, and GaAs (with band gaps of 1.1−1.4 eV), do not produce sufficient voltage to drive the water-splitting reaction since the practical energy input needed for water-splitting ranges from 1.6 to 2.3 eV (1.23 eV being the thermodynamic potential)[5] (Figure 1a).Thus, an external electrical bias is usually applied to provide the extra overpotential required to drive the water splitting reaction. Additionally, in order for a single-gap semiconductor electrode to do photoactivated water splitting, the conduction band (E_{cb}) and valence band (E_{vb}) edges of the semiconductor must straddle the water reduction and water oxidation potentials (Figure 1a).[1] This requirement then excludes most of the common semiconductor materials, such as $GaInP_2$ and GaP with ideal band gap, from achieving self-sustaining water-splitting. As a result, there are only few semiconductor materials that could meet requirements with the right energetics and band gap, such as Cu_2O and TiO_2 (Figure 1a). Previous studies with p-Cu_2O yielded high H_2 evolution Faradaic efficiencies, but the material is unstable due to the band edge positions of Cu_2O straddling the Cu(I) reduction and oxidation potentials.[6] TiO_2 has a large band gap and requires activation under UV light, making it nonideal for solar hydrogen production because UV light only accounts for <5% energy of the solar spectrum.[7]

Received: July 17, 2017
Revised: October 11, 2017
Accepted: October 17, 2017
Published: October 17, 2017

DOI: 10.1021/acs.est.7b03644
Environ. Sci. Technol. 2017, 51, 13494−13501

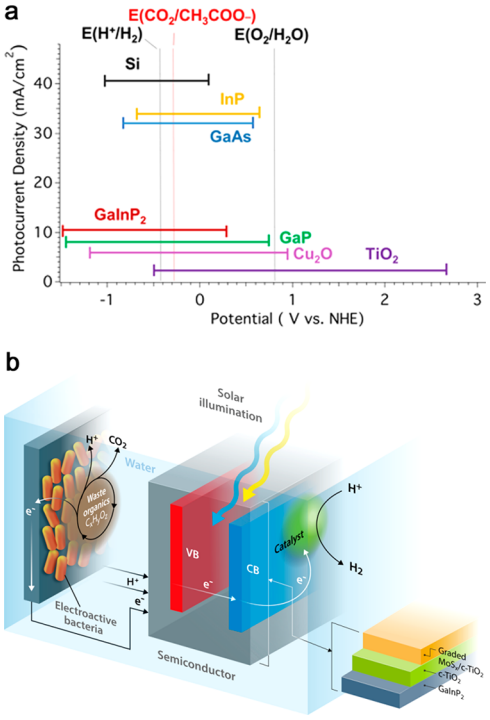

Figure 1. Schematic of band positions of common semiconductors and a microbial photoelectrosynthesis (MPES) system. (a) Conduction (left bar, E_{cb}) and valence band (right bar, E_{vb}) positions vs NHE of semiconductor materials used in photoelectrochemical reduction studies under conditions of pH = 7, T = 298.15 K, P = 1 atm. Here the band-gaps of Si, InP, GaAs, $GaInP_2$, GaP, Cu_2O, and TiO_2 materials are 1.1 eV, 1.3 eV, 1.4 eV, 1.8 eV, 2.3 eV, 2.4 eV, and 3.2 eV, respectively. The maximum theoretical photocurrent is under 1 sun condition (100 mW/cm^2). The black dotted lines are the thermodynamic potentials for water reduction and oxidation. The red dotted line is the thermodynamic potential of acetate (organic) oxidation. (b) Proposed self-sustaining MPES system with integrated microbial electrochemical oxidation and photoelectrochemical reduction.

To expand the availability of semiconductor materials for water-splitting, many approaches have been tried to eliminate the utilization of an external bias and improve material performance. Unassisted PEC cells have been built by employing multiple absorbing semiconductors (monolithic or nanostructured) with wired or multijunction configurations under parallel or tandem arrangements.[8−14] Dye-sensitized solar cells (DSSCs)[15−18] and perovskite solar cells (PSCs)[19,20] were also integrated into systems for unassisted solar water-splitting. However, complexity and limited device lifetime are still challenges for commercialization of these unbiased systems, in addition to some which require prolonged and expensive fabrication processes.

Microbial electrochemical oxidation (MEO) has emerged recently to recover electron and energy from organic substrate.[21,22] In this process, electroactive bacteria (EAB) capable of extracellular electron transfer oxidize organics and transfer electrons to an electrode (Figure 1b). The electrons can then be harvested as direct current or used to reduce protons to H_2 or CO_2 to organic molecules, respectively. EAB grow firmly as biofilm on the anode and serve as biocatalysts to boost oxidation reactions by employing multi cellular enzymes. Because MEO utilizes the chemical energy embedded in organics, much less energy is required than for water oxidation. For example, the potential of acetate degradation by MEO is only −0.285 V (vs normal hydrogen electrode, NHE, pH = 7, T = 298.15 K, P = 1 atm), which requires 1.1 V less energy input than 0.816 V for water oxidation under the same condition. In the water splitting reaction, the water oxidation half-reaction for electron generation is the rate limiting step due to the difficulties of mediating the 4-electron 4-proton transfer to produce molecular oxygen. If a MEO is used to replace water oxidation for coupling with water reduction, then the result is a negative shift of thermodynamic potential of oxidation, thus most semiconductors can be easily adopted for H_2 evolution without the need of external bias (Figure 1a). This reduces the requirements of semiconductors in terms of both band gap and redox energetics in an APS. MEO has other advantages compared to water oxidation, such as, (i) more stable oxidation reaction due to mild microbial process under normal biological conditions in temperature and organic loading, which could maintain stable for years; (ii) Low-cost carbon-based anode materials; (iii) no O_2 generation thereby eliminating O_2/H_2 separation; and (iv) environmental benefits can be earned such as wastewater treatment and carbon-emission alleviation. While some specific organic compounds, such as alcohols and organic acids, can be used as sacrificial reagents or hole scavengers in a photocatalytic reaction, this is different than the microbial electrochemical oxidation of organics,[23] because only chemicals with low oxidation potentials can be utilized as sacrificial donors. However, an electroactive bacterial consortium has been shown that can take up any complicated organic compounds contained in real wastewaters and generate current.[24,25] Moreover, the use of wastewater greatly expands the applicability of APS as wastewater is generated anywhere human being are present and need energy, and it is free, readily available, and abundant. This approach also enables energy-efficient wastewater treatment, as current wastewater treatment processes are energy intensive and consume 2−4% of global electricity production.[26] The conversion of the chemical energy in the wastewater, which is multiple times the energy used in treatment, can transform wastewater treatment from energy-intensive to energy-positive and subsequently reduce carbon-emission.[27] Qian et al. have shown that a pure culture of *Shewanella oneidensis* MR-1could be coupled with *p*-Cu_2O nanowire photocathode to generate current under zero electric bias, but the slow electron transfer dynamics on the anode and the nature of *p*-Cu_2O (fast charge recombination, rapid corrosion rate, and small photocurrent production) led to very low current density (0.05 mA/cm^2).[28] In addition, the use of pure culture may not be practical for treatment of actual wastewater. Another study demonstrated the use of a microbial fuel cell (MFC) with MEO on the anode to drive a traditional photoelectrochemical cell (PEC) for self-based hydrogen production, but it didn't investigate the direct coupling of MEO with a semiconductor cathode.[29]

Here, an integrated microbial photoelectrosynthesis (MPES) approach was used to enable energy-efficient, self-sustaining hydrogen evolution from artificial wastewater (Figures 1 and S1 of the Supporting Information, SI). A natural mixed culture from an indigenous environment harvests electrons from organic matter and delivers them to a carbon anode. The electrons are then transported to a p-type semiconductor $GaInP_2$ to combine with the holes in valence band upon light illumination, while photogenerated electrons at the conduction band reduce protons in the electrolyte. The back contacts of the $GaInP_2$ electrode were made by electron-beam evaporation

DOI: 10.1021/acs.est.7b03644
Environ. Sci. Technol. 2017, 51, 13494−13501

of a layer of titanium (10 nm) for the better attachment of the Au layer, followed by 300 nm of gold deposition. An annealed bilayer of protective amorphous titanium (TiO_x) and catalytic molybdenum sulfide (MoS_x) was deposited onto $GaInP_2$ for efficient and stable H_2 production. The MPES performance in terms of HER and stability was investigated under unassisted and applied bias conditions.

MATERIALS AND METHODS

$GaInP_2$−TiO_2−MoS_x Photocathode Preparation. Epilayer of *p*-$GaInP_2$ was grown on *p*-GaAs(100) substrates, miscutting toward (111) phase by 4° in an organometallic vapor-phase epitaxy technique.[30] The p-type doping level of $GaInP_2$ is about 2×10^{17} by Zn. Back contacts were created by electron-beam evaporation of 10 nm of titanium, followed by 300 nm of gold on top of the GaAs. The ohmic contacts were made by attaching copper wires through silver paste (PELCO colloid silver) followed by covering the whole electrode with glass and sealed with two layer of epoxy consequently (first layer of Loctite 9462 Hysol and second layer of Loctite E-120 HP) at room temperature for overnight.

The deposition method for TiO_x, PtRu, and MoS_x onto the $GaInP_2$ was described in our previously published procedure.[31] In this study, a layer of amorphous titanium dioxide (TiO_x) and cost-effective amorphous molybdenum sulfide (MoS_x) catalyst thin film were successively deposited onto $GaInP_2$ to serve as productive and catalytic layer, respectively, Amorphous molybdenum sulfide (MoS_x) thin film was deposited onto the TiO_x layer by reductive electrodeposition (−0.3 V vs Ag/AgCl). The electrode was annealed at 450 °C to form a highly active and graded MoS_x/c-TiO_2 catalyst layer, which demonstrated outstanding stability and catalytic efficiency toward hydrogen evolution in acidic condition.[31] The thickness of TiO_2 layer was 24−30 nm based on STEM characterization. The HER catalyst loading amounts of MoS_2 and PtRu are 10.49 and 3.5 nmol/cm^2, respectively. The surface area of photocathodes was measured between 0.081 to 0.09 cm^2.

IPCE Measurement. Incident photon-to-current efficiency (IPCE) was performed in a three-electrode configuration. Ag/AgCl served as the reference electrode and Pt foil was the counter electrode in a 1 M phosphate buffer (pH 7) solution at 0 V versus RHE. The setup details can be found in our previous studies.[30] Each plot was gained by the average value of two experiments.

Bioanode Enrichment and Growth Medium Preparation. Bioanodes made of carbon fiber brush (2.5 cm diameter and 2.5 cm length, 0.22 m^2 surface area) were first acclimated in a three-electrode electrochemical cell with a poised anode potential of 0 V (vs Ag/AgCl electrode, Pt counter electrode).[32] Anaerobic sludge obtained from an anaerobic digester was used as microbial inoculum. The electrochemical cell was fed with artificial wastewater ($NaCH_3COO$, 1.5 g/L; Na_2HPO_4, 4.58 g/L; $NaH_2PO_4{\cdot}H_2O$, 2.45 g/L; NH_4Cl, 0.31 g/L; KCl, 0.13 g/L; trace mineral and vitamin solution; pH = 7.0; and conductivity = 8.0 mS/cm)[33] for growth. The electrochemical cell was operated in fed-batch mode with replacement of substrate medium in each batch until stable electric current was generated. After that, the enriched bioanodes were transferred to single-chamber photoelectrochemical reactors (3 cm diameter and 6 cm length) (SI Figure S1) for coupled investigation with photocathode.

Microbial Photoelectrosynthesis Measurement. For each reactor, the bioanode and photocathode were placed on the opposite ends of the reactor with a distance of 3 cm. The effective liquid volume of each reactor was 40 mL (Figure S1). The reactors were fed with nitrogen gas sparged artificial wastewater to maintain their anaerobic condition and were operated in fed-batch mode. A 150 W tungsten-halogen lamp coupled with a UV-IR cut filter (sharp cutoff below 400 nm and above 700 nm) that blocks infrared irradiation was used as the solar simulator. The intensity of the light was calibrated by a $GaInP_2$ photodiode to ensure an incident photo density identical to 1-sun (100 mW/cm^2). A potentiostat (Biologic VMP3) was used for bias (0 to −0.8 V) application to the photocathode (vs anode) and linear sweep voltammetry (LSV) measurement. The self-sustaining MPES (without bias) was performed by applying a 0 V bias, in which the potentiostat served as an ammeter. For convenience, all applied bias and associated currents were reported as positive values. Ag/AgCl electrodes (BASi-RE-5B, 0.197 V vs SHE) were used as reference, and coiled platinum wires (BASi-MW-1033) were used as counter electrodes. The difference in potential across the electrodes was recorded by a data acquisition system (model 2700, Keithley). H_2 produced at the photocathode was collected in the headspace via a glass tube connected with the reactor, and gas content was measured using a gas chromatograph (Model 8610C, SRI Instruments) equipped with a thermal conductivity detector. Chemical oxygen demand (COD) of wastewater was measured using a standard method (HACH Company). MPES durability tests were performed in a 24-h period without anode substrate limitation. A control microbial electrolysis cell (MEC) was constructed by replacing photocathode with a glassy carbon electrode (BASi- MF-2012, 0.071 cm^2 projected surface area) coated with 2.56 μmol/cm platinum (10% Pt on Vulcan XC72), and its H_2 production was compared with MPES reactors.

RESULTS AND DISCUSSION

Photoelectrochemical Profile of Photocathode. The p-type semiconductor $GaInP_2$ was used as the light absorber due to its ideal direct band gap of 1.8 eV and excellent electronic transport properties. Our previous study showed that conversion of a bilayer of amorphous MoS_x/TiO_x to a graded *g*-$MoS_x/MoO_yS_z/MoO/c$-TiO_2 catalytic-protection layer resulted in a photocathode with a higher stability for the HER than $GaInP_2$ coupled with a PtRu alloy catalyst, while retaining much of the high catalytic activity of amorphous MoS_x in strong acid solution (0.5 M H_2SO_4).[31] However, the photoelectrochemical properties of $GaInP_2$−TiO_2−MoS_x photoelectrode under biological condition in neutral solution (pH = 7) are unknown. Representative photocurrent density-potential curves for $GaInP_2$−TiO_2−MoS_x and $GaInP_2$−PtRu electrodes in neutral solution are shown in Figure S2a. The $GaInP_2$−PtRu photoelectrode demonstrated a slightly better performance than the $GaInP_2$−TiO_2−MoS_x in terms of a more positive onset potential (0.5 versus 0.4 V (vs RHE)) and a higher current density (1.44 versus1.08 mA/cm^2) at zero overpotential. Overall though, both photoelectrodes showed very close photoelectrochemical properties, which indicates a low cost catalyst could replace the Pt−Ru catalyst for efficient hydrogen generation.[31]

The real-time applied bias between the photoelectrodes and Pt counter electrode during potential scans was measured and the value ranged from 0.82 to 2.56 V (Figures S2a and S3). This indicates that a high electrical energy input is needed to operate this PEC cell with a single-band photocathode in pH =

DOI: 10.1021/acs.est.7b03644
Environ. Sci. Technol. 2017, 51, 13494−13501

7 electrolyte. This effect is usually ignored in a photoelectrode's characterization and optimization process. For example, a 2.56 V bias must be applied to a $GaInP_2$−TiO_2−MoS_x electrode in order to reach a current density of 10 mA/cm^2. Integration of an electroactive bioanode with a photocathode can significantly reduce the external bias/input energy needed while maintaining high current density (for discussion see following section). The $GaInP_2$−TiO_2−MoS_x electrode displayed a high incident phototo-current conversion efficiency (IPCE) of up to 80% across the visible range (Figure S2b), ∼18% higher than the $GaInP_2$−PtRu electrode, and ∼31% higher than the bare $GaInP_2$. $GaInP_2$−TiO_2 demonstrates a poor ability to convert photon into electron, which is consistent with its well-known poor visible light photocurrent response.[30]

Integration of Bioanode with Photocathode for Photocurrent Generation. Electroactive bioanodes were enriched using a natural mixed culture from an indigenous environment. The mixed culture takes advantage of the syntrophy between electroactive bacteria (EAB) and other functional microbial communities so comparing with a pure culture a diverse range of substrates (e.g., proteins, carbohydrates, organic acids, and hydrocarbons)[24,25] can be utilized, high resilience to environmental changes can be accomplished,[34] and systems related to real-world applications can be developed.[35] Cyclic voltammetry (CV) was employed to evaluate the electrochemical activity of these bioanodes (Figure S4). The CV showed that the bioanodes produced a far higher current than a bare carbon brush anode without the bacteria, indicating the conversion of organic substrates to electrons by the electroactive bioanode.

To validate the concept of microbial photoelectrosynthesis (MPES), we connected a bioanode with a photocathode via a potentiostat and applied a bias ranging from 0 to −0.8 V vs the anode (Figure 2a, b). For convenience, all applied bias and associated currents are reported as positive values. At 0 V bias, both the $GaInP_2$−TiO_2−MoS_x and $GaInP_2$−PtRu photocathodes generated a short-circuit current density of 0.55 and 0.59 mA/cm^2 (potentiostat serves as an amperemeter here), respectively, under light illumination, indicating the system is self-sustaining, operating unassisted. The photocurrent dramatically increased when a small bias was applied. The current density reached to a maximum of 10.8 ($GaInP_2$−TiO_2−MoS_x) and 12.1 mA/cm^2 ($GaInP_2$−PtRu) at only 0.8 V bias, which is 1.76 V or 69% less than the photocathode with Pt counter electrode (Figure S2a). Note that there was no current production in the dark at any bias. Moreover, integration of an abiotic anode (bare carbon brush) or a platinum anode with photocathodes only generated negligible current at high bias (0.6−0.8 V) under illumination. In practice, this small bias can be provided by many renewable energy sources, with an example a microbial fuel cell (MFC),[21,29] which is an electrochemical cell that can be constructed using similar bioanode to convert organic waste into electricity. An additional benefit of MPES is that this hybrid bioassisted photoelectrochmical structure allows the decoupling of hydrogen evolution from water oxidation rather associated with organic oxidation. This further permits process advancement by enabling independent reaction optimization and utilization of different organic compounds with various redox properties, so energy efficiency can be further improved.

The MPES performance was compared with another H_2 production technology microbial electrolysis cell (MEC), which was identified as a key route for biological H_2 generation from

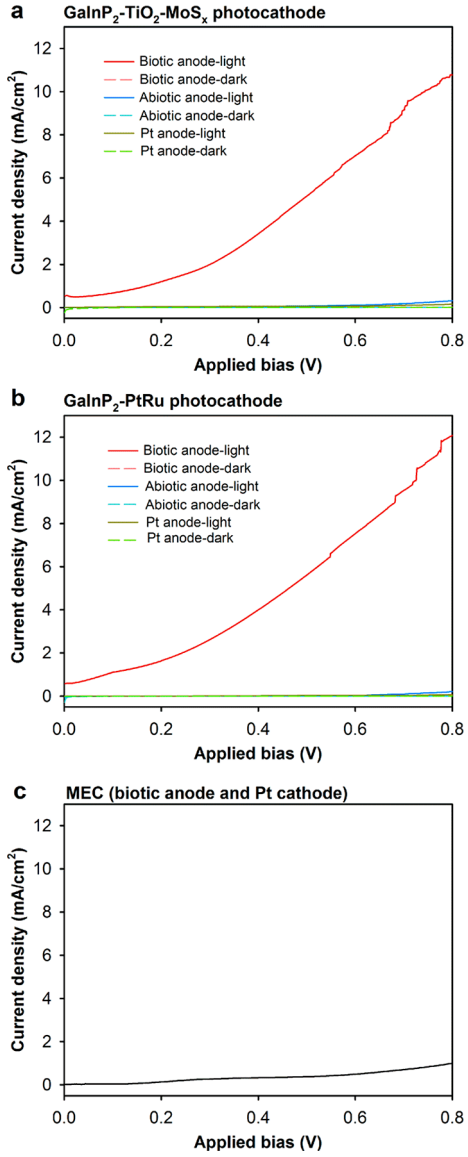

Figure 2. Current density versus applied bias curves in MPES and MEC systems. (a, b) Photocurrent density-applied bias curves for microbial photoelectrosynthesis (MPES) systems with $GaInP_2$−TiO_2−MoS_x and $GaInP_2$−PtRu photoelectrode, respectively (in pH 7 buffer solution under 1 sun (100 mW/cm^2) illumination). External bias (10 mV/s step) was applied between different anodes and photocathodes. Abiotic anode shares the same electrode as biotic anode but without bacteria on it. (c) Current density-applied bias curves for microbial electrolysis cell (MEC) show much lower current outputs.

biomass by the US Department of Energy.[25,36] The MEC was equipped with the same bioanode but a Pt cathode for electrochemical proton reduction. Figure 2c demonstrates that no current was generated at 0 V bias from the MEC, while a minimal current of 1.0 mA/cm^2 was generated under a 0.8 V bias. Compared with 12.1 mA/cm^2 generated by MPES, this current is an order of magnitude lower. This indicates that the integration of bioanode and photocathode demonstrates great potential for more efficient water-splitting and hydrogen evolution.

To investigate the short time durability of the hybrid system, I−t curves of MPES under dark and illumination conditions (each lasts 10 min) were examined (Figure 3). Under self-

DOI: 10.1021/acs.est.7b03644
Environ. Sci. Technol. 2017, 51, 13494−13501

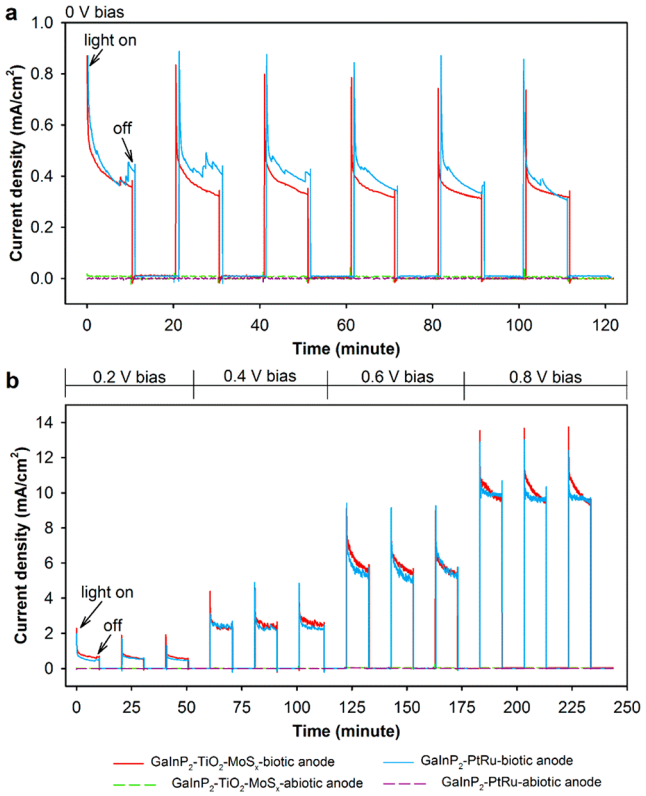

Figure 3. Photocurrent density versus time of MPES without and with external bias. (a) Comparison of photocurrent densities of MPESs with two photoelectrodes upon on/off 1 sun illuminations (100 mW/cm^2) under self-sustaining condition (0 bias) or (b) 0.2−0.8 V bias in pH 7 buffer solution. Abiotic anode shares the same electrode as biotic anode but without bacteria on it.

sustaining condition, obvious photocurrent generation was observed once the photocathode was illuminated. The photocurrent then sharply declined to a relatively stable level (around 0.4 mA/cm^2) due to capacitance change on the photocathode.[37] The $GaInP_2$−PtRu electrode displayed a slightly higher photocurrent than the $GaInP_2$−TiO_2−MoS_x. When the illumination on the photocathode was blocked, the current dropped to almost zero. Active MPES showed a very stable reproducibility for the photocurrent-illumination response, while photocathodes coupled with abiotic anodes always generated zero current. Under bias condition, the photocurrent has a strongly positive correlation with applied bias, which is consistent with the values obtained by potential scan given in Figure 2. Both photocathodes have similar current profiles and demonstrated repeated response to illumination. The photoinduced potential change of the bioanode and the photocathode under open circuit condition were also measured (Figure S5). The potential of bioanode is almost constant at around −0.48 V vs Ag/AgCl with or without illumination, while $GaInP_2$−TiO_2−MoS_x and $GaInP_2$−PtRu photoelectrodes exhibited about 0.6 and 0.2 V photoresponse, respectively, which leads to the open circuit voltages of 1.08 ($GaInP_2$−TiO_2−MoS_x) and 0.68 ($GaInP_2$−PtRu) V. The increased open circuit voltage may result from the formation of a p−n solid junction (p-$GaInP_2$/n-TiO_2), which produces an internal electric field that increases the operating photovoltage and improves photo induced charge separation across the semiconductor to the catalysts interface.[2,38]

Overall Stability of MPES. In addition to short-term (10 min) I−t curves, longer-term (24 h) durability was also characterized to evaluate system stability and scale up potential (Figure 4). At 0 V bias (self-sustaining condition), the

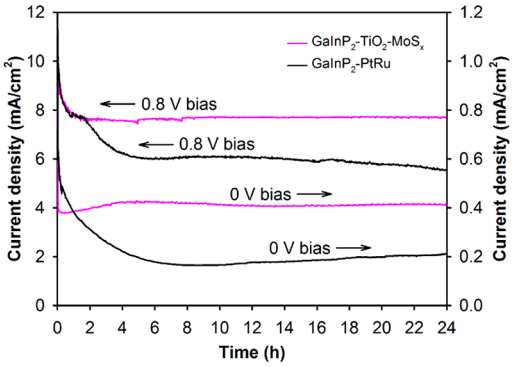

Figure 4. Stability test of current production in MPES. 24-h photocurrent density versus time curves of MPESs with two photoelectrodes at 0 and 0.8 V bias in pH 7 buffer solution under 1 sun (100 mW/cm^2) illumination.

photocurrent density of the $GaInP_2$−TiO_2−MoS_x electrode displayed a similar drop in the first few minutes as in the short term tests owing to capacitance change. The current then increased to reach a plateau at 0.42 mA/cm^2, which is consistent with the value in the short term I−t curve. However, the photocurrent density of the $GaInP_2$−PtRu electrode continuously decreased from 0.8 to 0.16 mA/cm^2 after 8 h, and then recovered to about 0.2 mA/cm^2 at the end of experiment, indicating a half decay compared to that obtained in short-term experiment. The same phenomenon has also been observed at 0.8 V bias. Both electrodes exhibited a decline in the photocurrent within the first 2 h, then the $GaInP_2$−TiO_2−MoS_x electrode stabilized at around 7.7 mA/cm^2 while the photocurrent of $GaInP_2$−PtRu continued to drop to 5.6 mA/cm^2 after 24 h, which represents a 23% and 44% decrease compared to an initial current of about 10 mA/cm^2. This decay of photocurrent should be derived from photocathodes rather than bioanode, because the current decay due to substrate limitation for anodic bacteria has been excluded by providing sufficient substrate (electron donor) for sustaining maximum current generation far longer than 24 h based on Coulombic calculation. In general, the cost-effective $GaInP_2$−TiO_2−MoS_x electrode is more stable than the precious metal modified $GaInP_2$−PtRu electrode due to a combination effect of TiO_2 protection layer and intercalated TiO_2−MoS_x catalytic layer, which agrees with results obtained for these electrodes in acid solution.[31] Interestingly, almost all decrease in photocurrent density for $GaInP_2$−TiO_2−MoS_x electrode in neutral solution occurred within the first 2 h, and then a stable profile was observed from 2 to 24 h. The initial decay of the photocathode under neutral condition is still under investigation. Hydrogen generation was confirmed by gas chromatography, which showed a high current to H_2 conversion recovery efficiency (Faradaic efficiency) of 93−97% (Table S1). For the condition with a 0.8 V bias, the energy efficiency was defined as a ratio of recovered energy in H_2 to the input electrical energy. Both photoelectrodes obtained an energy efficiency of 178−180% (Table S1), indicating that MPES gained almost twice energy (H_2 energy) as much as the consumed electrical energy.

DOI: 10.1021/acs.est.7b03644
Environ. Sci. Technol. 2017, 51, 13494−13501

Table 1. Self-Sustaining Photoelectrochemical Systems for Water-Splitting[a]

light absorber	current density (mA/cm^2)	stability (hour)	reference
$GaInP_2$/GaAs tandem solar cell	120 (12 sun)	0.5	9
triple-junction amorphous silicon	3.5	0.5	44
Fe_2O_3/DSSC tandem	0.95	10	16
WO_3/DSSC tandem	2.52		
$BiVO_4$/WO_3/DSSC tandem	4.5	2	17
P−InGaN/*p*-GaN−InGaN/*n*-GaN/*n*-Si nanowire tandem		0.1	45
p-Cu−Ti−O nanotube with *n*-TiO_2	0.25		11
P−Si with *n*-WO_3/W	0.12	0.1	46
$Zn_xCd_{1-x}Se$ with *n*-$BiVO_4$	0.02 (1.2 sun)	0.1	47
p-Cu_2O/Cu_2S with *n*-ZnO/CdS	0.4	1.5	48
p-Si with *n*-Fe_2O_3	0.7	10	10
p-Si with *n*-$BiVO_4$	0.6	3.5	49
P−Si nanowire with *n*-TiO_2 nanorod	0.4	1.5	12
bioanode with $GaInP_2$−TiO_2−MoS_x	0.42	24	This study

[a]1 sun illumination except note.

Prospects and Challenges. The incorporation of microbial electrochemical oxidation significantly reduces the thermodynamic requirement for the oxidation half-reaction and electron generation potential. This greatly expands the range of semiconductors that can be used for H_2 generation from water-splitting despite smaller band-gaps or E_{cb} positions. Moreover, new semiconductors can be developed with more negative E_{cb} but with a similar band gap, which will lead to higher potential for reduction reactions in MPES with visible light absorption.

The proof-of-concept MPES with mixed culture bioanode and $GaInP_2$−TiO_2−MoS_x photocathode showed comparable photocurrent density generation (0.42 mA/cm^2) with the performance obtained in traditional unassisted PEC cells with two wired electrodes (0.02−0.7 mA/cm^2, Table 1). The key challenges for coupling two separate photocathodes and photoanodes are that both electrodes should have (1) appropriate band edge position, (2) high charge separation efficiency, (3) prolonged stability, and (4) ideally coupled photocurrent density. Typically, even with a single semiconductor it is difficult to achieve all of the above requirements, so having two electrodes with matched current density and optimized properties is extremely difficult. While a few tandem PEC cells with multijunction configurations have displayed higher performance, the crystallinity of the semiconductor with suitable band energetics, the interfacial electronic properties in the heterojunction, and the absorption properties of each material need to be considered carefully in the design. Thus, the fabrication complexity and stability are still critical challenges for these devices, which also lead to high cost.[39] Our MPES showed a 24 h long-term stability for photocurrent generation, which is more durable than other self-sustaining PEC cells (∼10 h). Previous results from our and other laboratories showed that bioanodes can be stable for years with minimal performance drop. The carbon fiber brush anode used here has a cost of only ∼\$0.05/m^2-surface area based on a recent quote and web site information,[40] which is negligible compared to the cost of regular semiconductor photoelectrode material silicon panels (cost ≈ \$400/m^2).

MPES demonstrates good potential for efficient water-splitting with low cost and high stability, and further advancements can be focused on photocurrent generation, especially under self-sustaining conditions. The individual photocathode and bioanode current−potential properties can be characterized independently, and with that the intersection of the two *J*−*V* curves at the maximum current density can be achieved under self-sustaining conditions (Figure S6). As shown in Figure S6, the photocathode and bioanode cross at −0.6 V (vs Ag/AgCl). Endeavors will be made to induce a negative shift of the bioanode *J*−*V* curve and a positive shift of the photocathode *J*−*V* curve so current generation at each electrode can be enhanced at the current intersection position. The bioanode surface area can be increased to harvest more electrons, while semiconductor materials and substrates can be optimized to improve onset potentials. The charge recombination rate can be reduced and the interfacial charge transfer can be increased by utilization of higher efficiency catalysts with higher charge transfer kinetics. Covering the cathode surface with a thin oxide protect layer to reduce surface recombination, and the use of capacitors to boost bioanode potential can also be adopted.[30,41−43] While an abundant hydrogen reaction evolution (HRE) catalyst MoS_x was used here to replace the noble metal catalyst Pt/Ru, a low-cost semiconductor, such as nanostructured Si, with a protective layer is currently under investigation for possible coupling to our MPES electrodes for the real wastewater treatment and fuel generation purposes. In addition, two-chamber configuration of MPES with highly efficient membrane separator can be adopted in future to relieve the impact of contaminants in real wastewaters on photocathode.

Sole abiotic PEC technologies laid out a grant vision that one only needs free sunlight and clean water to generate enough energy for household self-use. Unfortunately, the process has been hindered by the performance of the anodic half reaction which in many cases did not match with the performance in the cathodic reaction. The MPES system enables the decoupling of the anodic reaction from oxygen evolution and instead accessing hundreds and thousands of organic oxidations that could be utilized to lower the overall energy requirement. Moreover, one associated challenge not mentioned in most artificial water splitting discussions is that many communities (nearly 3 billion people or 40% of world population) do not have access to clean water or sanitation. In this regard, wastewater energy processes such as MPES can provide many mutual benefits, because not only can some sanitation issues be addressed but also the autonomy of artificial photosynthesis can be realized by taking advantage of the energy recovered from household wastewater.

DOI: 10.1021/acs.est.7b03644
Environ. Sci. Technol. 2017, 51, 13494−13501

■ ASSOCIATED CONTENT

Supporting Information

The Supporting Information is available free of charge on the ACS Publications website at DOI: 10.1021/acs.est.7b03644.

Digital pictures of the MPES reactors (Figure S1); photoelectrochemical measurements of $GaInP_2$-based photoelectrodes for H_2 evolution (Figure S2); potential of Pt counter electrode and applied bias (between Pt counter electrode and photocathode) during linear sweep of photocathodes (Figure S3); cyclic voltammograms of abiotic and biotic anode under turn-over (with substrate) and non-turn-over (without substrate) conditions (Figure S4); open-circuit potential of the bioanode and $GaInP_2$ based photocathode (Figure S5); overlaid current-potential behavior for photocathodes and a bioanode (Figure S6); calculations of coulombic, faradaic and energy efficiencies; and performance of MPES in terms of COD removal, H_2 production, Coulombic efficiency, Faradaic efficiency, and energy efficiency during long-term (24 h) experiments (Table S1) (PDF)

■ AUTHOR INFORMATION

Corresponding Authors

*E-mail: jgu@sdsu.edu (J.G.).
*E-mail: zhiyong.ren@colorado.edu (J.R.).

ORCID

Zhiyong Jason Ren: 0000-0001-7606-0331

Author Contributions

L.L. did the microbial electrode fabrication. N.B.W. and J.G. did the photocathode fabrication and characterizations. L.L. and Z.Y.J.R. did the MPES characterization. J.T. and P.C.M. contribute to the initial design of experiment, providing the materials, and trouble shootings in the experiments. L.L., Z.Y.J.R., J.G., J.T., and P.C.M. wrote the manuscript. The authors in the manuscript want to thank Alfred Hicks for drawing the artistic picture in Figure [1], for this manuscript. The data are available upon request. There is no competing interests between the authors.

Notes

The authors declare no competing financial interest.

■ ACKNOWLEDGMENTS

L.L. and Z.J.R. were supported by the US National Science Foundation (NSF) under Award CEBT-1510682. J.G. and N.B.W. were funded by SDSU startup funds, the SDSU University Grants Program, and NSF award CEBT-1510681.

■ REFERENCES

(1) Walter, M. G.; Warren, E. L.; McKone, J. R.; Boettcher, S. W.; Mi, Q.; Santori, E. A.; Lewis, N. S. Solar water splitting cells. *Chem. Rev.* **2010**, *110* (11), 6446−6473.

(2) Yang, Y.; Gu, J.; Young, J. L.; Miller, E. M.; Turner, J. A.; Neale, N. R.; Beard, M. C. Semiconductor interfacial carrier dynamics via photoinduced electric fields. *Science* **2015**, *350* (6264), 1061−1065.

(3) Kim, D.; Sakimoto, K. K.; Hong, D.; Yang, P. Artificial photosynthesis for sustainable fuel and chemical production. *Angew. Chem., Int. Ed.* **2015**, *54* (11), 3259−3266.

(4) Wen, F.; Li, C. Hybrid artificial photosynthetic systems comprising semiconductors as light harvesters and biomimetic complexes as molecular cocatalysts. *Acc. Chem. Res.* **2013**, *46* (11), 2355−2364.

(5) Turner, J. A. A realizable renewable energy future. *Science* **1999**, *285* (5428), 687−689.

(6) Paracchino, A.; Laporte, V.; Sivula, K.; Grätzel, M.; Thimsen, E. Highly active oxide photocathode for photoelectrochemical water reduction. *Nat. Mater.* **2011**, *10* (6), 456−461.

(7) Giese, A. C. *Photophysiology: Current Topics in Photobiology and Photochemistry*; Elsevier: Amsterdam, 2013.

(8) Ding, C.; Qin, W.; Wang, N.; Liu, G.; Wang, Z.; Yan, P.; Shi, J.; Li, C. Solar-to-hydrogen efficiency exceeding 2.5% achieved for overall water splitting with an all earth-abundant dual-photoelectrode. *Phys. Chem. Chem. Phys.* **2014**, *16* (29), 15608−15614.

(9) Khaselev, O.; Turner, J. A. A monolithic photovoltaic-photoelectrochemical device for hydrogen production via water splitting. *Science* **1998**, *280* (5362), 425−427.

(10) Jang, J.-W.; Du, C.; Ye, Y.; Lin, Y.; Yao, X.; Thorne, J.; Liu, E.; McMahon, G.; Zhu, J.; Javey, A. Enabling unassisted solar water splitting by iron oxide and silicon. *Nat. Commun.* **2015**, *6*, 7447.

(11) Mor, G. K.; Varghese, O. K.; Wilke, R. H.; Sharma, S.; Shankar, K.; Latempa, T. J.; Choi, K.-S.; Grimes, C. A. p-Type Cu−Ti−O nanotube arrays and their use in self-biased heterojunction photoelectrochemical diodes for hydrogen generation. *Nano Lett.* **2008**, *8* (7), 1906−1911.

(12) Liu, C.; Tang, J.; Chen, H. M.; Liu, B.; Yang, P. A fully integrated nanosystem of semiconductor nanowires for direct solar water splitting. *Nano Lett.* **2013**, *13* (6), 2989−2992.

(13) Shaner, M. R.; McDowell, M. T.; Pien, A.; Atwater, H. A.; Lewis, N. S. Si/TiO_2 tandem-junction microwire arrays for unassisted solar-driven water splitting. *J. Electrochem. Soc.* **2016**, *163* (5), H261−H264.

(14) Yang, H. B.; Miao, J.; Hung, S.-F.; Huo, F.; Chen, H. M.; Liu, B. Stable quantum dot photoelectrolysis cell for unassisted visible light solar water splitting. *ACS Nano* **2014**, *8* (10), 10403−10413.

(15) Kim, J. K.; Shin, K.; Cho, S. M.; Lee, T.-W.; Park, J. H. Synthesis of transparent mesoporous tungsten trioxide films with enhanced photoelectrochemical response: application to unassisted solar water splitting. *Energy Environ. Sci.* **2011**, *4* (4), 1465−1470.

(16) Brillet, J.; Yum, J.-H.; Cornuz, M.; Hisatomi, T.; Solarska, R.; Augustynski, J.; Graetzel, M.; Sivula, K. Highly efficient water splitting by a dual-absorber tandem cell. *Nat. Photonics* **2012**, *6* (12), 824−828.

(17) Shi, X.; Zhang, K.; Shin, K.; Ma, M.; Kwon, J.; Choi, I. T.; Kim, J. K.; Kim, H. K.; Wang, D. H.; Park, J. H. Unassisted photoelectrochemical water splitting beyond 5.7% solar-to-hydrogen conversion efficiency by a wireless monolithic photoanode/dye-sensitised solar cell tandem device. *Nano Energy* **2015**, *13*, 182−191.

(18) Shi, X.; Jeong, H.; Oh, S. J.; Ma, M.; Zhang, K.; Kwon, J.; Choi, I. T.; Choi, I. Y.; Kim, H. K.; Kim, J. K. Unassisted photoelectrochemical water splitting exceeding 7% solar-to-hydrogen conversion efficiency using photon recycling. *Nat. Commun.* **2016**, *7*, 11943.

(19) Kim, J. H.; Jo, Y.; Kim, J. H.; Jang, J. W.; Kang, H. J.; Lee, Y. H.; Kim, D. S.; Jun, Y.; Lee, J. S. Wireless solar water splitting device with robust cobalt-catalyzed, dual-doped $BiVO_4$ photoanode and perovskite solar cell in tandem: a dual absorber artificial leaf. *ACS Nano* **2015**, *9* (12), 11820−11829.

(20) Da, P.; Cha, M.; Sun, L.; Wu, Y.; Wang, Z.-S.; Zheng, G. High-performance perovskite photoanode enabled by Ni passivation and catalysis. *Nano Lett.* **2015**, *15* (5), 3452−3457.

(21) Wang, H.; Ren, Z. J. A comprehensive review of microbial electrochemical systems as a platform technology. *Biotechnol. Adv.* **2013**, *31* (8), 1796−1807.

(22) Logan, B. E. Exoelectrogenic bacteria that power microbial fuel cells. *Nat. Rev. Microbiol.* **2009**, *7* (5), 375−381.

(23) Schneider, J.; Bahnemann, D. W. Undesired role of sacrificial reagents in photocatalysis. *J. Phys. Chem. Lett.* **2013**, *4*, 3479−3483.

(24) Lu, L.; Xing, D.; Ren, Z. J. Microbial Community Structure Accompanied with Electricity Production in A Constructed Wetland Plant Microbial Fuel Cell. *Bioresour. Technol.* **2015**, *195*, 115−121.

(25) Lu, L.; Ren, Z. J. Microbial electrolysis cells for waste biorefinery: A state of the art review. *Bioresour. Technol.* **2016**, *215*, 254−264.

DOI: 10.1021/acs.est.7b03644
Environ. Sci. Technol. 2017, 51, 13494−13501

(26) Lu, L.; Huang, Z.; Rau, G. H.; Ren, Z. J. Microbial electrolytic carbon capture for carbon negative and energy positive wastewater treatment. *Environ. Sci. Technol.* **2015**, *49* (13), 8193−8201.
(27) Heidrich, E.; Curtis, T.; Dolfing, J. Determination of the internal chemical energy of wastewater. *Environ. Sci. Technol.* **2011**, *45* (2), 827−832.
(28) Qian, F.; Wang, G.; Li, Y. Solar-driven microbial photoelectrochemical cells with a nanowire photocathode. *Nano Lett.* **2010**, *10* (11), 4686−4691.
(29) Wang, H.; Qian, F.; Wang, G.; Jiao, Y.; He, Z.; Li, Y. Self-biased solar-microbial device for sustainable hydrogen generation. *ACS Nano* **2013**, *7* (10), 8728−8735.
(30) Gu, J.; Yan, Y.; Young, J. L.; Steirer, K. X.; Neale, N. R.; Turner, J. A. Water reduction by a p-$GaInP_2$ photoelectrode stabilized by an amorphous TiO_2 coating and a molecular cobalt catalyst. *Nat. Mater.* **2015**, *15* (4), 456−460.
(31) Gu, J.; Aguiar, J. A.; Ferrere, S.; Steirer, K. X.; Yan, Y.; Xiao, C.; Young, J. L.; Al-Jassim, M.; Neale, N. R.; Turner, J. A. A graded catalytic−protective layer for an efficient and stable water-splitting photocathode. *Nat. Energy* **2017**, *2*, 16192.
(32) Wang, X.; Zhou, L.; Lu, L.; Lobo, F. L.; Li, N.; Wang, H.; Park, J.; Ren, Z. J. Alternating current influences anaerobic electroactive biofilm activity. *Environ. Sci. Technol.* **2016**, *50* (17), 9169−9176.
(33) Lu, L.; Hou, D.; Wang, X.; Jassby, D.; Ren, Z. J. Active H_2 harvesting prevents methanogenesis in microbial electrolysis cells. *Environ. Sci. Technol. Lett.* **2016**, *3* (8), 286−290.
(34) Lu, L.; Ren, N.; Zhao, X.; Wang, H.; Wu, D.; Xing, D. Hydrogen production, methanogen inhibition and microbial community structures in psychrophilic single-chamber microbial electrolysis cells. *Energy Environ. Sci.* **2011**, *4* (4), 1329−1336.
(35) Li, W.-W.; Yu, H.-Q.; He, Z. Towards sustainable wastewater treatment by using microbial fuel cells-centered technologies. *Energy Environ. Sci.* **2014**, *7* (3), 911−924.
(36) Randolph, K.; Studer, S. *2013 Biological Hydrogen Production Workshop Summary Report, U.S.*; Department of Energy, Office of Energy Efficiency and Renewable Energy, Fuel Cell Technologies Office: 2013.
(37) Bard, A. J.; Faulkner, L. R.; Leddy, J.; Zoski, C. G. *Electrochemical methods: fundamentals and applications*. Wiley: New York, 1980; Vol. *2*.
(38) Digdaya, I. A.; Han, L.; Buijs, T. W.; Zeman, M.; Dam, B.; Smets, A. H.; Smith, W. A. Extracting large photovoltages from a-SiC photocathodes with an amorphous TiO_2 front surface field layer for solar hydrogen evolution. *Energy Environ. Sci.* **2015**, *8* (5), 1585−1593.
(39) Peerakiatkhajohn, P.; Yun, J.-H.; Wang, S.; Wang, L. Review of recent progress in unassisted photoelectrochemical water splitting: from material modification to configuration design. *J. Photonics Energy* **2017**, *7* (1), 012006−012006.
(40) Wang, X.; Cheng, S.; Feng, Y.; Merrill, M. D.; Saito, T.; Logan, B. E. Use of carbon mesh anodes and the effect of different pretreatment methods on power production in microbial fuel cells. *Environ. Sci. Technol.* **2009**, *43* (17), 6870−6874.
(41) Brown, P. R.; Kim, D.; Lunt, R. R.; Zhao, N.; Bawendi, M. G.; Grossman, J. C.; Bulović, V. Energy level modification in lead sulfide quantum dot thin films through ligand exchange. *ACS Nano* **2014**, *8* (6), 5863−5872.
(42) Alaraj, M.; Ren, Z. J.; Park, J. Microbial Fuel Cell Energy Harvesting using Synchronous Flyback Converter. *J. Power Sources* **2014**, *247*, 636−642.
(43) Lobo, F. L.; Wang, H.; Forrestal, C.; Ren, Z. J. AC Power Generation from Microbial Fuel Cells. *J. Power Sources* **2015**, No. 297, 252−259.
(44) Reece, S. Y.; Hamel, J. A.; Sung, K.; Jarvi, T. D.; Esswein, A. J.; Pijpers, J. J.; Nocera, D. G. Wireless solar water splitting using silicon-based semiconductors and earth-abundant catalysts. *Science* **2011**, *334* (6056), 645−648.
(45) AlOtaibi, B.; Fan, S.; Vanka, S.; Kibria, M.; Mi, Z. A metal-nitride nanowire dual-photoelectrode device for unassisted solar-to-hydrogen conversion under parallel illumination. *Nano Lett.* **2015**, *15* (10), 6821−6828.
(46) Chen, Q.; Li, J.; Li, X.; Huang, K.; Zhou, B.; Shangguan, W. Self-biasing photoelectrochemical cell for spontaneous overall water splitting under visible-light Illumination. *ChemSusChem* **2013**, *6* (7), 1276−1281.
(47) Park, H. S.; Lee, H. C.; Leonard, K. C.; Liu, G.; Bard, A. J. Unbiased photoelectrochemical water splitting in Z-scheme device using W/Mo-doped $BiVO_4$ and $Zn_xCd_{1-x}Se$. *ChemPhysChem* **2013**, *14* (10), 2277−2287.
(48) Bai, Z.; Zhang, Y. A Cu_2O/Cu_2S-ZnO/CdS tandem photoelectrochemical cell for self-driven solar water splitting. *J. Alloys Compd.* **2017**, *698*, 133−140.
(49) Xu, P.; Feng, J.; Fang, T.; Zhao, X.; Li, Z.; Zou, Z. Photoelectrochemical cell for unassisted overall solar water splitting using a $BiVO_4$ photoanode and Si nanoarray photocathode. *RSC Adv.* **2016**, *6* (12), 9905−9910.

DOI: 10.1021/acs.est.7b03644
Environ. Sci. Technol. 2017, 51, 13494−13501